Araştırma Makalesi / Research Article

Structural-crystalline, optical, topographical properties of ZnO thin film produced in presence of various oxygen

Asim MANTARCI*

Opticianry Department, Muş Alparslan University, Muş, Turkey
(ORCID: 0000-0001-8369-3559)

Abstract
Changes in growth conditions of ZnO thin films produced in the presence of different oxygen, changes in important properties such as crystal, surface properties, and absorption properties of the films were examined and reported. It is inferred from the XRD experimental results that the oxygen we applied to the films plays a role in the crystal structure changes of the films (grain size, strain value, dislocation density, etc.). The highest value of RMS roughness of the film is 8.58 nm and the lowest value of RMS roughness of the film is 1.08 nm, which corresponds to non-flow and 1 sccm flow film, respectively. AFM proved that films with nano-structured, tightly packed, grain properties were obtained in the produced films. Inference from UV analysis made is that the oxygen applied to the film caused small changes in the optical band gap values (in the range of about 3.30-3.32 eV). Except for 3 sccm oxygen state, all the films obtained were tightly packed, granulated and almost homogeneous and the nano property was clearly seen. All the results obtained show that the oxygen applied in the ZnO film process causes some changes in the physical properties of the film and this has an effect on the film quality and it is seen that these results can contribute to the production of ZnO thin film-based Light Emitting Diodes (LEDs).

Keywords: ZnO, Oxygen, SEM, Nano property, dislocation density.

Çeşitli oksijen varlığında üretilen ZnO ince filmin yapısal kristal, optik, topografik özellikleri

Öz
Farklı oksijen varlığında üretilen ZnO ince filmlerin büyüme koşullarındaki değişiklikler, filmlerin kristal, yüzey özellikleri ve soğurma özellikleri gibi önemli özellikleri üzerindeki değişiklikler incelenmiş ve raporlanmıştır. XRD deneysel sonuçlarından, filmlere uyguladığımız oksijenin filmlerin kristal yapı değişikliklerinde (tane boyutu, gerinim değeri, dislokasyon yoğunluğu vb.) rol oynadığı anlaşılmaktadır. Filmin en yüksek RMS pürüzlülüğü değeri 8.58 nm'dir ve filmin en düşük RMS pürüzlülüğü değeri 1.08 nm'dir, bu değerler sırasıyla akışsız ve 1 sccm akışlı filme karşılık gelir. AFM, üretilen filmlerde nano yapılı, sıkı paketlenmiş, tanecik özellikli filmler elde edildiğini kanıtladı. Filmlerin UV analizinden, uygulanan oksijenin filmlerin optik bant aralığı enerjisinde (yaklaşık 3.30-3.32 eV aralığında) küçük değişikliklere sebep olduğu gözlenmiştir. 3 sccm oksijen durumu dışında, elde edilen tüm filmler sıkıca paketlenmiş, tanecik yapılı ve neredeyse homojen olan ve nano özelliği açıkça görüldü. Elde edilen tüm sonuçlar, ZnO film işleminde uygulanan oksijenin filmin fiziksel özelliklerinde bir takım değişikliklere neden olduğunu ve bunun film kalitesine etki ettiğini göstermektedir ve bu sonuçların ZnO ince film tabanlı ışık yayan diyot cihazlarının (LED) üretimine katkı sağlayabileceği görülmüştür.

Anahtar kelimeler: ZnO, Oksijen, SEM, Nano özellik, Dislokasyon yoğunuğu.

1. Introduction

The ZnO film attracts the attention of many researchers due to its use in high-tech industrial products including piezoelectric nano-generators [1], Uv-photodetector [2], polymer-solar cell [3], memory device [4]. The features that make this material the reason for preference are given as follows; such as the bonding energy at room temperature 60 meV, wide direct optical bandgap energy (about 3.30 eV), high thermal stability, high electrochemical stability, low cost, non-toxicity, abundance in nature [5-8].

*Corresponding author: asimmantarci@gmail.com
Received: 24.02.2021, Accepted: 03.05.2021

Therefore, ZnO thin film has become very good candidate for optoelectronic device application thanks to above features. The researcher [9] was done a study about indium impacts on ZnO film's physical characterization. Also, the importance of UHV process to stimulate incorporation into the ZnO matrix has been demonstrated. Measurements and analyzes of AES, XPS, UPS and PL were made for the examination of the thin film. From XPS analysis, core-level peaks of Zn 2s, Zn 2p, In 3p, O 1s, In 3d, C 1s, Zn 3s, Zn 3p, Zn 3d, and Auger transition peaks Zn LMM, In MNN, and O KLL were found in this study. Also, it was found carbon is present on the surfaces as a contamination layer confirmed by its high at % (47.98% for UZO and 52.02% for IZO). PL analysis showed that incorporation of indium into the clean ZnO matrix increases the level of Z_{ni} and V_{Zn} defects inducing a broadening in the NBE emission. Other report [10] investigates Bi+3 effects on ZnO film's photoelectrical parameters. In this study, how photo-current generation mechanism of Bi +3-doped the film work was investigated. Good photoelectric parameter values were obtained at different doping densities. They found that 1% Bi3+ doped BZO thin film has better photoelectric properties. Under the simulated 1.5 G sunlight, the photocurrent density of 1% Bi3+ doped BZO thin film was sharply increased and then reached to 2.5 μA/cm2 constant states. In addition, it was obtained that for BZO thin films; the absorption at around 400 nm can be distinguished compared with pure ZnO film. It was achieved that Bi3+ doped BZO thin films showed that its charge transfer resistance was significantly less than that of pure ZnO thin film. In this project, the variation of detailed physical parameters of ZnO films produced using radio-frequency-magnetron sputter technique in the presence of different oxygen was investigated. SEM, AFM, XRD, UV measurements of advanced characterization techniques were taken for different oxygen values and analyzed. The unique aspect of the study is that besides the application of oxygen to the film, the change in the physical parameters of the film has not been studied; the results obtained may contribute to the production of optoelectronic devices.

2. Material and Methods

2.1. Film Processing

The sputtering technique used to grow films can be summarized briefly as directing energetic ions towards the target in the plasma environment. The way this technique works can be given as follows; the ions strike the target atoms, the atoms scatter from the surface of the target, and these scattered atoms move towards the substrate surface and settle there. There are basically two types of sputtering modes known as DC and RF sputtering. Conductive materials are studied in DC mode, non-conductive materials are studied in RF mode. In addition, an important point is that thanks to the magnet used in RF magnetron sputtering, the material is ionized better in the electric and magnetic field and turns into plasma form. RF magnetron sputter was executed in the DAYTAM research center. Target used ZnO (purity: 4N 99.9999%, thickness: 2 * 1.25 inc), purchased from ACI company. The substrates p-Si (100) orientation came from sigma chemical company. First of all, the substrates were cleaned by RCA-1 and RCA-2 methods [11]. Target and substrate were placed in their proper places in the system. Then the system was taken to the initial pressure. Then, 60 sccm argon working gas was given to the system. Plasma was formed by giving power. In the first stage, pre-sputtering was done for 6 minutes so that the surface was cleaned. The film processing parameters applied are listed in Table 1. Film processing was done DAYTAM in the clean room. While each film was being grown, non-flow, 1, 2, 3, 4 sccm oxygen was applied separately. Thicknesses were measured with the help of P-7 KLA tensor after films and it was found to be approximately 120 nm (with 3 nm error).

Table 1. Film processing parameters

Oxygen (sccm)	RF Power (W)	Base Pressure (kPa)	Working Pressure (kPa)	Growth Rate (A°/s)	Substrate Temperature (C°)
Non-flow	60	0.12×10^{-6}	0.81×10^{-3}	0.3	300
1	60	0.23×10^{-6}	0.85×10^{-3}	0.3	300
2	60	1.17×10^{-6}	0.89×10^{-3}	0.2	300
3	60	1.16×10^{-6}	0.82×10^{-3}	0.3	300
4	60	0.37×10^{-6}	0.86×10^{-3}	0.2	300

2.1. Film Characterizations

The characterization of the films was completed with SEM, AFM, XRD and absorption measurements (UV) in the measurement laboratory within DAYTAM. SEM measurements were carried out to investigate the surface properties of the films. Before SEM measurement, films were coated with 4 nm gold to allow measurement. SEM (Zeiss-300) measurements were taken in the secondary electron mode and taken at 80.84 KX, 90.00 KX, 114.11 KX, 90.89 KX, 100.00 KX magnifications. XRD measurement was used to examine the crystal and detailed structure parameters of the films. The panalytical D-8 XRD system with CuK_{α}=1.5406 A° was used for diffraction measurement. The measurement was taken between 10^{o} and 80^{o} degrees and at room temperature, depending on the intensity-2Θ. Topographic-surface properties (roughness etc.) of the films were investigated with the help of AFM. 500II-AFM system with tapping mode was executed for topography analysis of material. Also, AFM measurements were taken in both 2 dimensions and 3 dimensions. The absorption properties of films and related parameters such as optical band gap energy were studied by UV absorption measurement. 1050-UV lambda was operated for absorption study at room temperature and 200-1100 nm wavelength.

3. Results and Discussions

3.1. Diffraction Analysis

Figure 1 clearly shows us the XRD diffraction behavior of thin films produced. As seen from this figure, $35.56°, 35.56°, 35.40°, 35.58°, 35.58°$ peaks were obtained in the presence of 0, 1, 2, 3, 4 sccm oxygen. These peaks correspond to the phase of the ZnO material (002) when viewed from the open crystallography system (with no: 10 11 258 COD) [12]. In addition, $64.35°, 64.35°, 64.18°, 64.37°, 64.37°$ peaks were also achieved. These peaks correspond to the phase of the ZnO material (103) when viewed from the open crystallography system [12]. The very intensity peak is the substrate peak, which is p-Si. The slight shifts in the peaks we obtain indicate the stress caused by film processing mistakes (such as impurities) and therefore in the film. The grain size of the films in varying oxygen flow can be calculated by means of the Debye Scherer formula [13];

$$Z = {t.\lambda}/{v.\cos\theta} \quad (1)$$

t is the constant, λ is X-ray wavelength, v is full width of half maximum value, θ infers angle of diffraction. Formula below gives us the dislocation density of the films;

$$\& = 1/Z^2 \quad (2)$$

The strain values in the internal structure of the films were calculated using the following formula;

$$\varepsilon = {v.\cos\theta}/{4} \quad (3)$$

It has been seen from the analysis that the grain size decreases from the no-flow film to 1 sccm flow film, while the strain values and dislocation density increase. But; the grain size increases from the 1 sccm film to 2 sccm flow film, while the strain values and dislocation density decrease. Furthermore, the grain size decreases from the 2 sccm film to 3 sccm flow film, while the strain values and dislocation density increase (Table 2). On the other hand; the grain size increases from the 3 sccm film to 4 sccm flow film, while the strain values and dislocation density decrease. The decrease/increase in grain size in the polycrystalline film in certain oxygen exchange may be due to the different oxygen resulting in an increase/decrease in the surface energy of the film and this is supported by the literature [14]. Herewith; it is inferred from the experimental results that the oxygen we applied to the films plays a role in the crystal structure changes of the films.

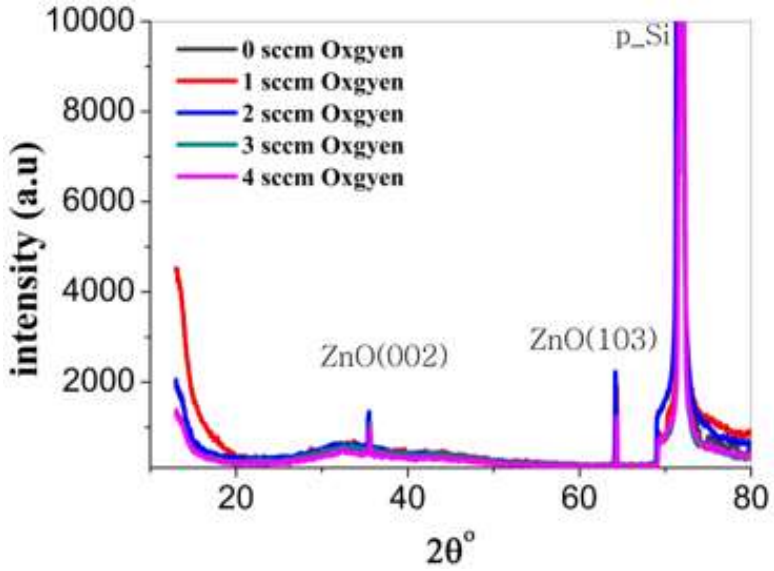

Figure 1. Diffraction graph of materials

Table 2. Crystal-structure properties of thin films produced

Oxygen Flow (sccm)	XRD Phase	FWHM (v) (°)	2θ (Observed) (°)	2θ (Theory) (°)	Dislocation density (&) (line.m^{-2})	Strain values (ε) (line^{-2}.m^{-4})	Grain size (Z)(nm)
Non-flow	(002)	0.69	35.56	34.46	0.00627	0.164	12.62
Non-flow	(103)	0.28	64.35	63.70	0.00081	0.059	35.00
1	(002)	0.71	35.56	34.46	0.00664	0.169	12.27
1	(103)	0.31	64.35	63.70	0.00100	0.065	31.61
2	(002)	0.68	35.40	34.46	0.00610	0.161	12.80
2	(103)	0.29	64.18	63.70	0.00087	0.061	33.76
3	(002)	0.72	35.58	34.46	0.00683	0.171	12.10
3	(103)	0.32	64.37	63.70	0.00106	0.067	30.63
4	(002)	0.75	35.58	34.46	0.00741	0.178	11.61
4	(103)	0.33	64.37	63.70	0.00113	0.069	29.70

3.2. Surface Topographical Analysis

Figure 2 gives the atomic force microscope (AFM) two and three dimensional pictures of the produced films. Figure 2 showed that highest the average slope was obtained as 29.03° in the non-flow film. But, lowest the average slope was obtained as 7.26° in the 1 sccm flow film. The film with the highest maximum depth is a non-flow film with 20.16 nm. The film with the lowest maximum depth is a 1 sccm flow film with 3.56 nm. The maximum height value of the film of 16.91 nm corresponds to a 2 sccm flow film. The lowest one of the film of 3.11 nm corresponds to a 1 sccm flow film. The highest RMS roughness value is 8.58 nm, the lowest RMS roughness value is 1.08 nm corresponding to non-flow and 1 sccm flow film respectively (see Figure 3). All values measured in the atomic force microscope can be found in Table 3. On the one hand, increasing from 1 sccm to 2 sccm and 3 sccm to 4 sccm increased the roughness to the film, resulting in a rougher surface. On the other hand, increasing from non-flow film to 1 sccm flow film and from 2 sccm to 3 sccm flow decreased the surface roughness and allowed us to obtain a smoother surface. In this study, ZnO material roughness value close to our values was obtained in the literature [15]. AFM proved that films with nano-structured, tightly packed, grain properties were obtained in the produced films. To come to the conclusion, oxygen application to films has changed the topography and surface properties of the films.

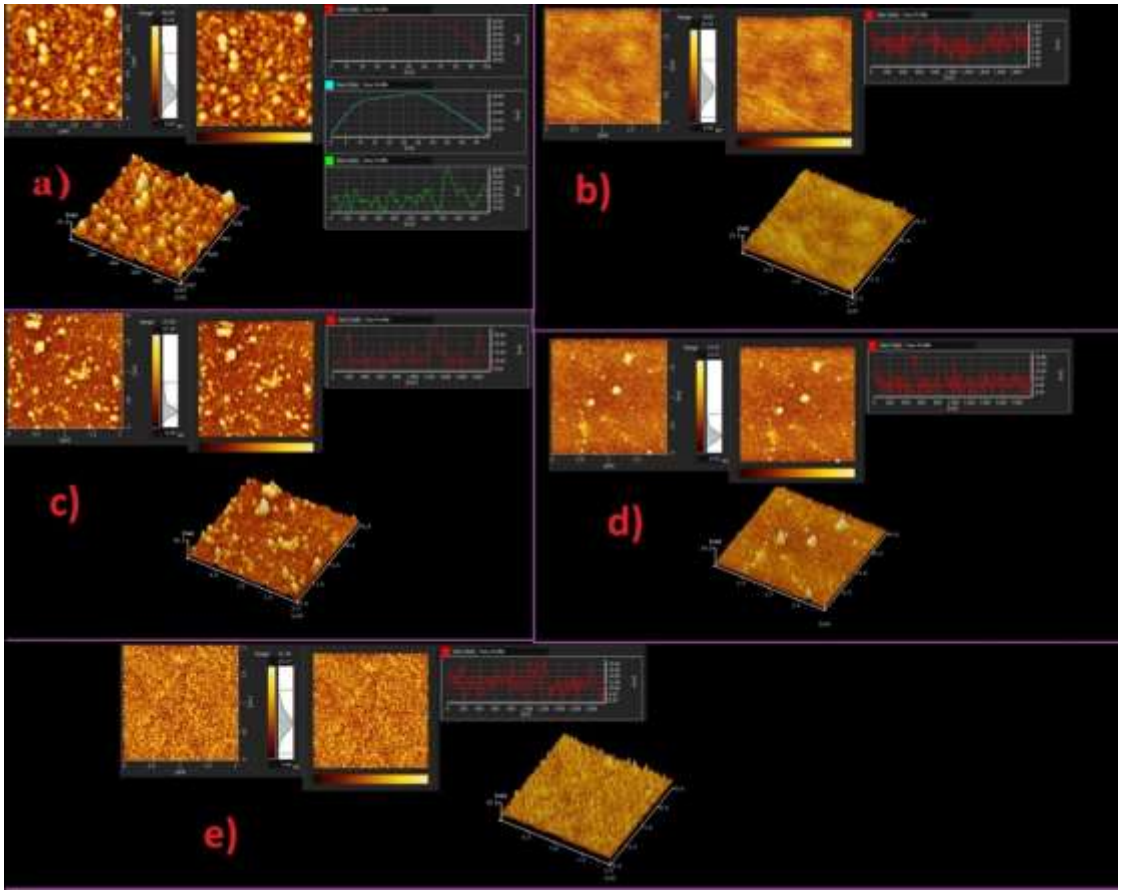

Figure 2. 2D-3D AFM pictures of materials at **a)** non-flow **b)** 1 **c)** 2 **d)** 3 **e)** 4 sccm oxygen

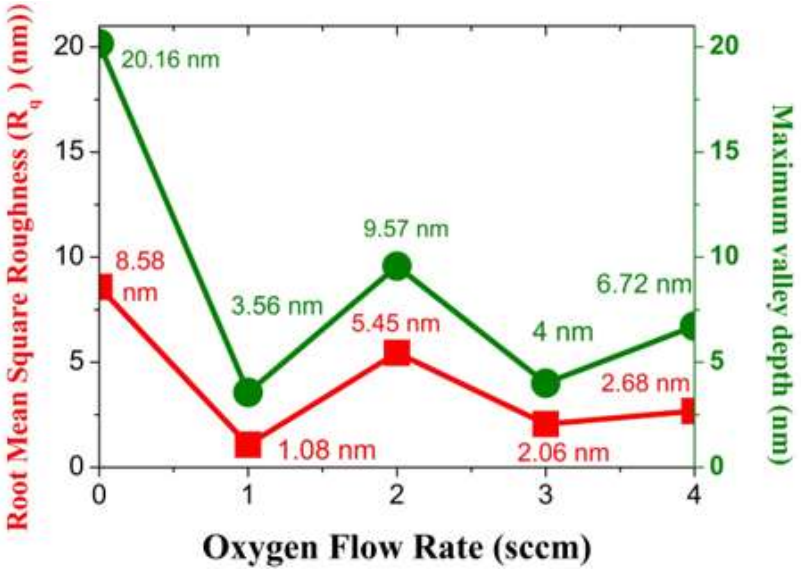

Figure 3. RMS Roughness and Maximum valley of materials

Table 3. Film processing parameters

Oxygen (sccm)	Average Roughness (R_a)(nm)	Maximum peak height (R_p)(nm)	Average absolute slope (Δa)(°)	Maximum valley Depth (R_v)(nm)	Root Mean Square Roughness (R_q)(nm)
Non flow	7.51	8.98	29.03	20.16	8.58
1	0.87	3.11	7.26	3.56	1.08
2	4.14	16.91	11.27	9.57	5.45
3	1.56	8.43	13.01	4.00	2.06
4	2.11	7.31	12.64	6.72	2.68

3.3. Scanning Electron Microscopy Analysis

When the SEM images of the films shown in Figure 4 are examined, it is clear that the almost homogeneous, granular, tightly packed structure of the films continue from the non-flow state to 1 sccm and from 1 sccm to 2 sccm. However, dislocations are noticeable on the surface of the films when the oxygen flow in the films is from 2 sccm to 3 sccm. These dislocations may cause cracks on the surface of the film and are therefore undesirable for our films. Afterwards, when the oxygen flow is from 3 sccm to 4 sccm, agglomeration occurs on the surface. Except for 3 sccm oxygen state, all the films obtained were tightly packed, granulated and almost homogeneous and the nano property was clearly seen. Similar SEM images in previous studies [16, 17] support our study.

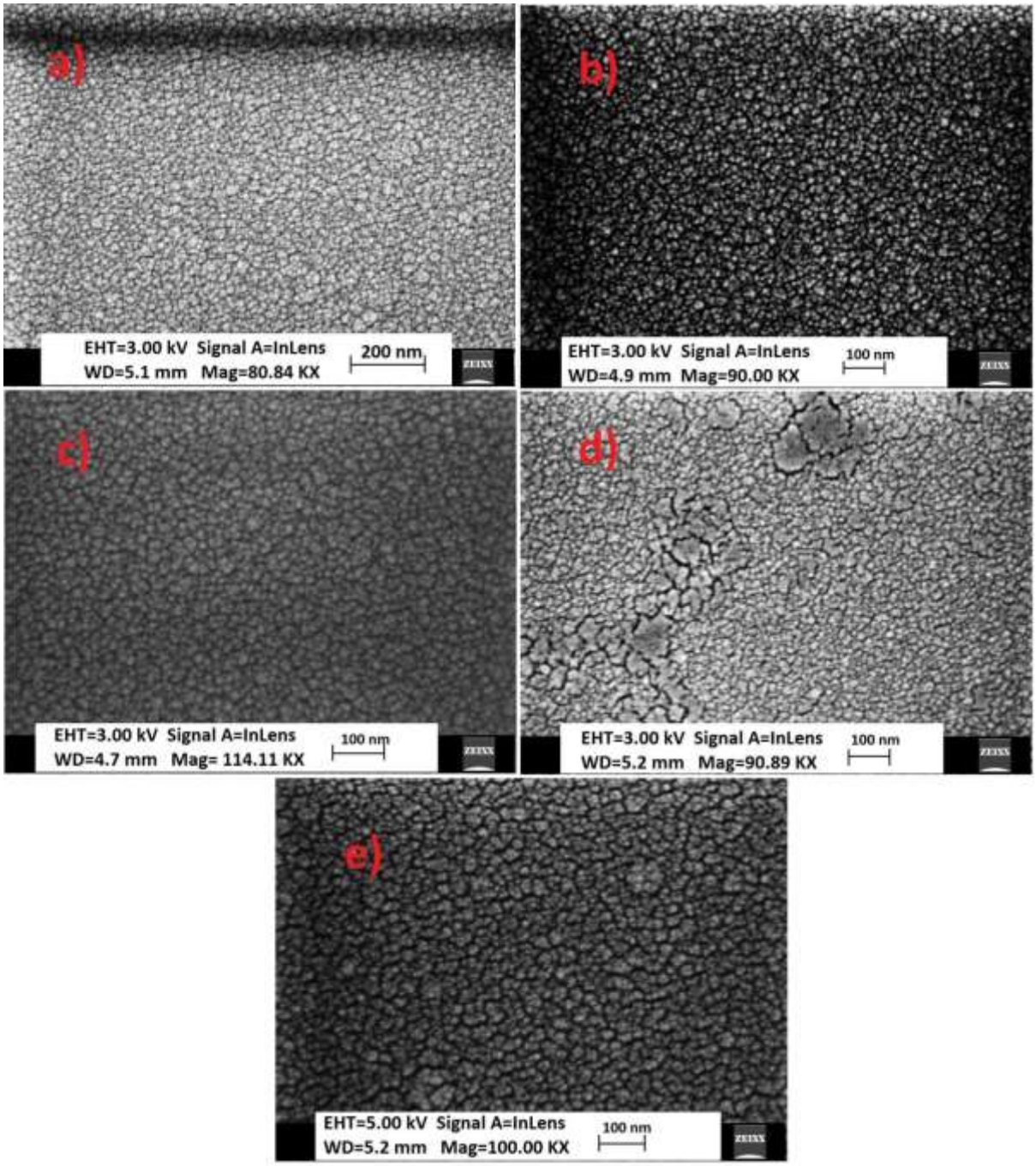

Figure 4. Pictures of SEM for materials at **a)** non-flow **b)** 1 **c)** 2 **d)** 3 **e)** 4 sccm oxygen

3.4. Absorption/UV Analysis

Figure 5 shows a plot of the corresponding photon energy to $(\alpha h\nu)^2$. If the following Tauc formula (4) is used in this graph, the value that cuts zero on the y-axis by taking n = 1/2 gives us the direct-allowed optical band gap energy of the films. Tauc formula is given;

$$(\alpha h\nu)^n = L(h\nu - E_g) \quad (4)$$

Where n shows band gap type, L shows the constant, hν shows photon energy, and E_g shows optical band gap energy of our materials. Material's E_g values were obtained as 3.3111, 3.3042, 3.3018, 3.3189, 3.3220 eV in the presence of no-flow, 1, 2, 3, 4 sccm oxygen. UV analysis proved optical band gap energy of films decreased when the flow was changed from non-flow film to the 1 sccm oxygen flow film and 1 sccm oxygen flow film to the 2 sccm oxygen flow film. Yet, it was observed that optical band gap energy value increased when the flow was changed from the 2 sccm oxygen film to the 3 sccm oxygen flow film and 3 sccm oxygen flow film to the 4 sccm oxygen flow film (Table 4). The literature study [18] supported us in this sense by finding a value close to optical band gap energy of ZnO. Inference from analysis made is that the oxygen applied to the film caused small changes in the optical band gap values.

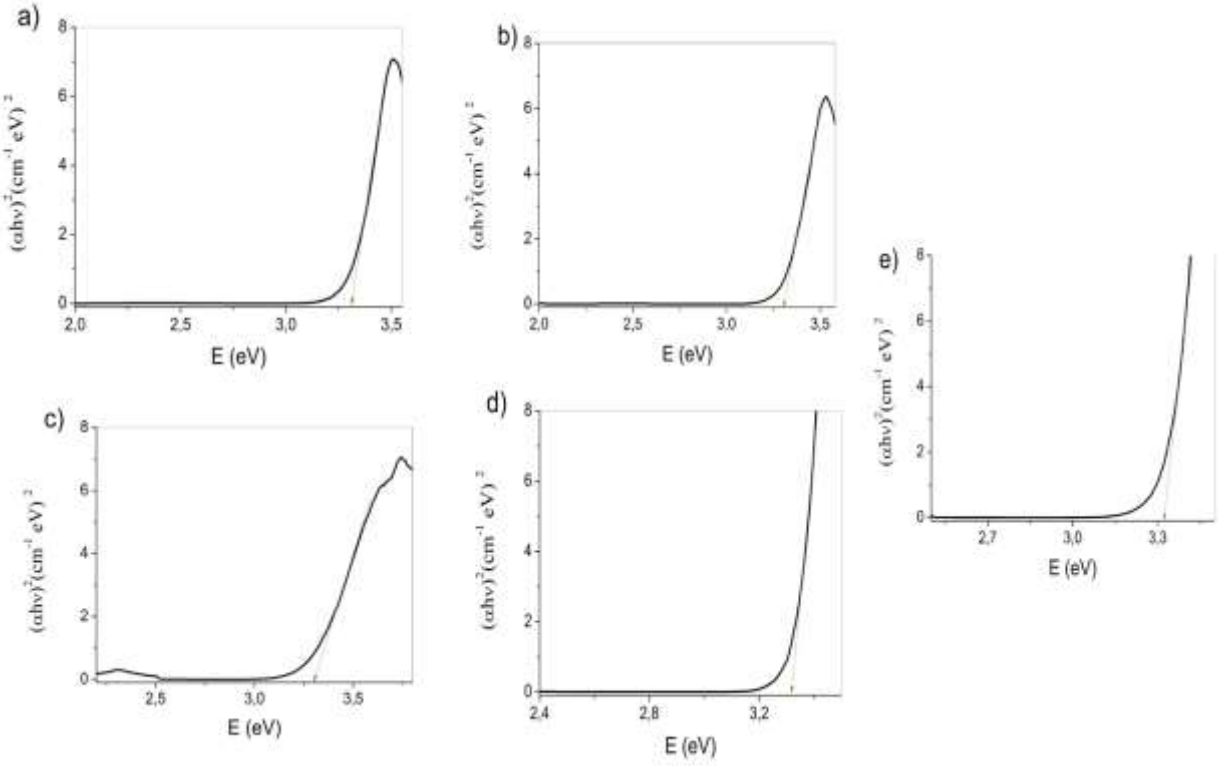

Figure 5. Absorption graph of materials at **a)** non-flow **b)** 1 **c)** 2 **d)** 3 **e)** 4 sccm oxygen

Table 4. Film's optical band gap energy values

Oxygen applied (sccm)	Optical band gap energy (eV)
Non flow	3.3111
1	3.3042
2	3.3018
3	3.3189
4	3.3220

4. Conclusions

Changes in growth conditions of ZnO thin films produced in the presence of different oxygen, changes in important properties such as crystal, surface properties, and absorption properties of the films were examined and reported. The phases of the ZnO material (002) and (103) were achieved from XRD study, proving ZnO has polycrystalline nature. It has been seen from the analysis that the grain size decreases from the non-flow film to 1 sccm flow film, while the strain values and dislocation density increase. But; the grain size increases from the 1 sccm film to 2 sccm flow film, while the strain values and dislocation density decrease. Herewith; it is inferred from the experimental results that the oxygen we applied to the films plays a role in the crystal structure changes of the films. It is clear that the almost homogeneous, granular, tightly packed structure of the films continue from the non-flow state to 1 sccm and from 1 sccm to 2 sccm. However, dislocations are noticeable on the surface of the films when the oxygen flow in the films is from 2 sccm to 3 sccm. These dislocations may cause cracks on the surface of the film and are therefore undesirable for our films. Material's E_g values were obtained as 3.3111, 3.3042, 3.3018, 3.3189, 3.3220 eV in the presence of non-flow, 1, 2, 3, 4 sccm oxygen, pointing out small changes in E_g values with applying oxygen. Highest the average slope was obtained as 29.03° in the non-flow film. But, lowest the average slope was obtained as 7.26° in the 1 sccm flow film. On the one hand, increasing from 1 sccm to 2 sccm and 3 sccm to 4 sccm increased the roughness to the film, resulting in a rougher surface. On the other hand, increasing from non-flow film to 1 sccm flow film and from 2 sccm to 3 sccm flow decreased the surface roughness and allowed us to obtain a smoother surface. All the results achieved show that the oxygen applied in the ZnO film process causes some changes in the physical properties of the film and this has an effect on the film quality and it is seen that these results can contribute to the production of ZnO thin film-based Light Emitting Diodes (LEDs).

Authors Contribution

All experimental, analysis, revision and all related procedures were carried out by Asim MANTARCI.

Statement of Conflicts of Interest

There is no conflict of interest.

Statement of Research and Publication Ethics

Research and publication ethics were followed in the study.

References

[1] Jin C., Hao N., Xu Z., Trase I., Nie Y., Dong L., Zhang J.X.J. 2020. Flexible piezoelectric nanogenerators using metal-doped ZnO-PVDF films. Sensors and Actuators A: Physical, 305: 111912.

[2] Zhang Y., Zhao X., Chen J., Li S., Yang W., Fang X. 2020. Self-Polarized BaTiO3 for Greatly Enhanced Performance of ZnO UV Photodetector by Regulating the Distribution of Electron Concentration. Advanced Functional Materials, 30 (5): 1907650.

[3] Bu F., Shen W., Zhang X., Wang Y., Belfiore L.A., Tang J. 2020. Hybrid ZnO Electron Transport Layer by Down Conversion Complexes for Dual Improvements of Photovoltaic and Stable Performances in Polymer Solar Cells. Nanomaterials, 10 (1): 80.

[4] Singh S.P., Sharma S.K., Kim D.Y. 2020. Carrier mechanism of ZnO nanoparticles-embedded PMMA nanocomposite organic bistable memory device. Solid State Sciences, 99: 106046.

[5] Al Dahoudi N. 2014. Comparative study of highly dense aluminium- and gallium-doped zinc oxide transparent conducting sol-gel thin films. Bulletin of Materials Science, 37 (6): 1243-1248.

[6] Muiva C.M., Sathiaraj T.S., Maabong K. 2011. Effect of doping concentration on the properties of aluminium doped zinc oxide thin films prepared by spray pyrolysis for transparent electrode applications. Ceramics International, 37 (2): 555-560.

[7] Lee J.-H., Ko K.-H., Park B.-O. 2003. Electrical and optical properties of ZnO transparent conducting films by the sol–gel method. Journal of Crystal Growth, 247 (1): 119-125.
[8] Sahal M., Hartiti B., Ridah A., Mollar M., Marí B. 2008. Structural, electrical and optical properties of ZnO thin films deposited by sol–gel method. Microelectronics Journal, 39 (12): 1425-1428.
[9] Bedrouni M., Kharroubi B., Ouerdane A., Bouslama M.H., Guezzoul M.H., Caudano Y., Abdelkrim M. 2021. Effect of indium incorporation, stimulated by UHV treatment, on the chemical, optical and electronic properties of ZnO thin film. Optical Materials, 111: 110560.
[10] Hou B., Li L., Li X., Li Q., Li J., Wang H., Huang J. 2021. Influence of Bi3+ doping on microstructure and photoelectric properties of ZnO thin film. Chemical Physics Letters, 763: 138174.
[11] Selman A.M., Hassan Z., Husham M. 2014. Structural and photoluminescence studies of rutile TiO2 nanorods prepared by chemical bath deposition method on Si substrates at different pH values. Measurement, 56: 155-162.
[12] http://www.crystallography.net/cod/index.php (Access Date: 20.02.2021).
[13] Patterson A.L. 1939. The Scherrer Formula for X-Ray Particle Size Determination. Physical Review, 56 (10): 978-982.
[14] Thompson C.V. 1990. Grain Growth in Thin Films. Annual Review of Materials Science, 20 (1): 245-268.
[15] Solookinejad G., Rozatian A.S.H., Habibi M.H. 2016. Zinc Oxide Thin Films Characterization, AFM, XRD and X-ray Reflectivity. Experimental Techniques, 40 (4): 1297-1306.
[16] O'Brien S., Koh L.H.K., Crean G.M. 2008. ZnO thin films prepared by a single step sol–gel process. Thin Solid Films, 516 (7): 1391-1395.
[17] Kim D., Woo H.K., Lee Y.M., Kim Y., Choi J.-H., Oh S.J. 2020. Controllable doping and passivation of ZnO thin films by surface chemistry modification to design low-cost and high-performance thin film transistors. Applied Surface Science, 509: 145289.
[18] Srikant V., Clarke D.R. 1998. On the optical band gap of zinc oxide. Journal of Applied Physics, 83 (10): 5447-5451.